Reaction Mechanisms in ^{56}Fe(p, p') from 5 to 6 MeV*

D. B. NICHOLS,† R. G. ARNS, H. J. HAUSMAN, AND R. G. SEYLER
The Ohio State University, Columbus, Ohio 43210
(Received 4 March 1969)

Proton angular distributions and spin-flip angular correlations have been measured as absolute cross sections for inelastic scattering of 4.96-, 5.58-, and 5.88-MeV protons to the first excited (2^+) state at 0.847 MeV in ^{56}Fe. The spin-flip measurements involve directional correlation of the 0.847-MeV γ rays, detected along a perpendicular to the reaction plane, with the inelastic protons observed at angles from 30° to 150° in the reaction plane. The spin-flip probability was determined for the three energies studied. The measured cross sections are compared with the predictions of the statistical model and the direct-interaction model. The compound-nucleus mechanism appears to dominate the reaction in this energy range. The statistical-model predictions, which are based on optical-model parameters obtained at somewhat higher energies, give the correct shape and order of magnitude, but fail to fit simultaneously both the angular distributions and the spin-flip correlation data.

I. INTRODUCTION

THE statistical compound-nucleus (CN) theory has provided a good description of inelastic nucleon scattering from medium-weight nuclei at incident energies $\lesssim$5 MeV. Model predictions have been experimentally verified in measurements of particle-γ correlations[1] and their energy dependence,[2] as well as in measurements of differential cross sections for scattered particles[3] and deexcitation γ rays.[4] At bombarding energies $\gtrsim$10 MeV,[5] on the other hand, the direct-interaction (DI) formalism is appropriate. For incident energies intermediate to these two domains, models of considerable recent interest have included both CN and DI contributions to calculated cross sections.[6,7]

The present work was undertaken in order to compare measured ^{56}Fe(p, $p'\gamma$) cross sections with CN predictions at several bombarding energies near the Coulomb barrier (~5.5 MeV), where DI mechanisms can be expected to have a detectable amplitude. A further objective was to see whether differences between the measurements and the CN predictions could be attributed to incoherent DI amplitudes. The results are presented in Secs. III and IV and are discussed in Sec. V.

The experimental measurement chosen for this comparison was that of spin-flip probability. Protons of laboratory energy 4.96, 5.58, and 5.88 MeV were inelastically scattered from ^{56}Fe (ground state $J^\pi=0^+$). Deexcitation-γ rays from the 0.847-MeV level ($J^\pi=2^+$) were detected in coincidence with the scattered protons. For this spin sequence a spin-flip correlation geometry was defined as that in which the γ-ray detector was fixed along a direction perpendicular to the reaction plane; the particle detector angle was a variable measured within the reaction plane. The spin-flip probability S involves both the absolute differential cross section for the scattered protons and the absolute double-differential cross section for the proton-γ correlation in the spin-flip geometry:

$$S=\frac{d^2\sigma(\phi_p,\theta_\gamma=0)}{d\Omega_p d\Omega_\gamma}\Big/\frac{d\sigma(\phi_p)}{d\Omega_p}W(\theta_\gamma=0).$$

The spherical coordinate system has the z axis along the reaction-plane normal. W is the distribution function for pure $l=2$, $m=\pm1$ γ radiation.

The interpretation of the quantity S as spin flip begins with a theorem due to Bohr[8]: If a two-body reaction is invariant under the operation of reflection through the reaction plane, then

$$P_i e^{i\pi S_i}=P_f e^{i\pi S_f},$$

where P_i and P_f are the intrinsic parities of the initial and final systems, and S_i and S_f are the sums of initial and final spin projections along a quantization axis perpendicular to the reaction plane. Schmidt *et al.* have then shown[9] that, for the present $0^+\to2^+\to0^+$ sequence, only transitions from the $m=\pm1$ magnetic substates of the 2^+ state can give γ radiation along the z axis. The $m=\pm1$ substates can be populated here only by proton spin flip. Hence, every 0.847-MeV level emitting a γ ray along the z axis has been populated by a proton undergoing spin flip.

With regard to model calculations, the statistical CN formalism gives spin-flip probability directly. Plane-wave direct-reaction theory predicts a spin-flip prob-

* Work supported in part by the National Science Foundation.
† Present address: California Institute of Technology, Kellogg Laboratory, Pasadena, Calif.
[1] R. M. Humes and H. J. Hausman, Phys. Rev. **139**, B846 (1965); H. Hulubei, A. Berinde, I. Neamu, N. Scintei, and N. Martalogu, Nucl. Phys. **89**, 165 (1966); M. P. Steiger, Helv. Phys. Acta **39**, 107 (1966).
[2] H. J. Hausman, R. M. Humes, and R. G. Seyler, Phys. Rev. **164**, 1407 (1967).
[3] J. H. Towle and W. B. Gilboy, Nucl. Phys. **72**, 515 (1965).
[4] D. B. Nichols and M. T. McEllistrem, Phys. Rev. **166**, 1074 (1968).
[5] H. E. Gove, in *Proceedings of the Rutherford Jubilee International Conference, Manchester, 1961*, edited by J. B. Birks (Heywood and Co. Ltd., London, 1961), p. 451.
[6] J. Hufner, C. Mahaux, and H. A. Weidenmuller, Nucl. Phys. **A105**, 489 (1967).
[7] K. F. Ratcliff and N. Austern, Ann. Phys. (N.Y.) **42**, 185 (1967).
[8] A. Bohr, Nucl. Phys. **10**, 486 (1959).
[9] F. H. Schmidt, R. E. Brown, J. B. Gerhart, and W. A. Kolasinski, Nucl. Phys. **52**, 353 (1964).

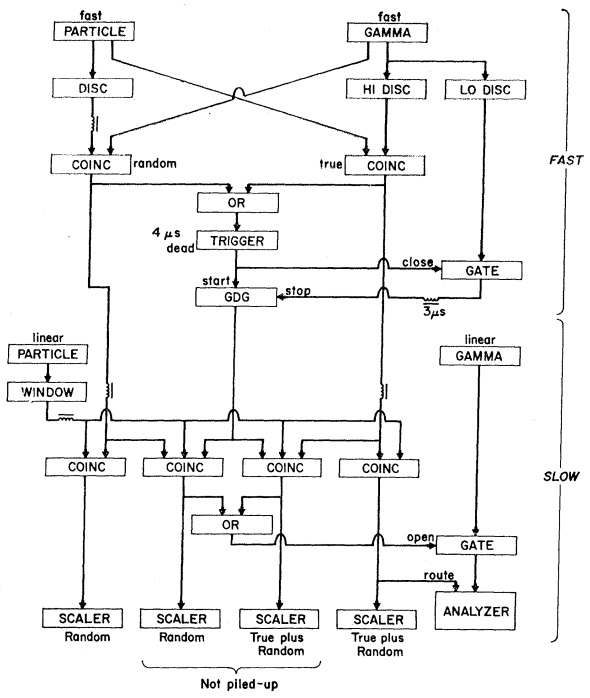

FIG. 1. Schematic diagram of the fast-slow coincidence circuit incorporating an interrogation circuit for determination of the pileup in the linear γ-ray signal.

ability only as related to a fitting parameter; under certain approximations the quantity S can be calculated. Incorporation of spin-orbit coupling and the collective-model extension of the optical model into the distorted-wave formalism also permits calculation of spin-flip probability. Spin-flip probability measurements can therefore serve not only to indicate the reaction mechanisms operative, but also to help delineate the spin-flip contribution to DI theory.

II. EXPERIMENTAL METHODS

Protons from the Ohio State University 5.5-MeV Van de Graaff accelerator were magnetically analyzed and directed into a scattering chamber which has been described elsewhere.[1] The hemispherical chamber had a radius of 12.7 cm and stainless-steel walls of thickness $\lesssim 0.16$ cm. Final collimation produced a beam 0.1 cm in diameter on target foils of self-supporting iron enriched to 99.7% in ^{56}Fe. The beam was stopped 17 cm beyond the target in a tantalum-lined Faraday cage equipped with electric field electron suppression. Scattered protons were detected in the reaction plane by a silicon surface-barrier detector positioned remotely to an angular accuracy of $\pm 0.1°$. The particle-detector solid angle was 4.09×10^{-3} sr for the correlation measurements and 4.00×10^{-4} sr for angular distributions.

A 7.62×7.62-cm NaI(Tl) crystal was located outside the chamber 13.5 cm from the target, along a direction perpendicular to the reaction plane. Chamber wall attenuation was 6.9% for 0.835-MeV γ rays. Photopeak detector efficiency was measured in the actual data-collection geometry by replacing the target with a ^{54}Mn point source; this γ ray differed from that studied in ^{56}Fe by only 12 keV. Uncertainties associated with the efficiency measurement were 1% in source calibration, 1.6% due to half-life uncertainty, and 0.6% due to positioning; the rms sum of these was 2%.

^{56}Fe target foils used were of two thicknesses: 0.90 and 2.70 mg/cm^2. Cross-section normalization was taken only from the heavier foil. Several measurements of proton energy loss were made using the ^{7}Li(p, n) threshold. Conversion to nuclei/cm^2 was made via the nine-parameter range formula of Barkas and Berger[10]; this expression is a least-squares fit of

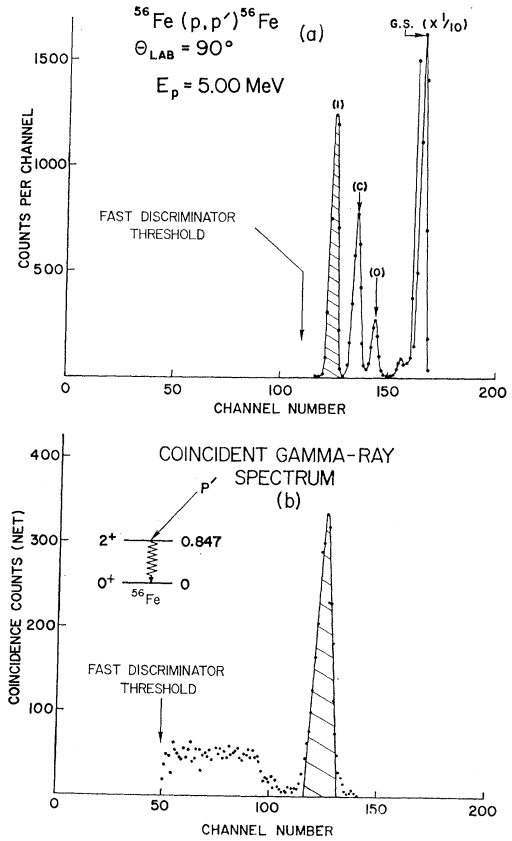

FIG. 2. (a) Proton spectrum from the ^{56}Fe(p,p') reaction measured at a laboratory angle of 90°. Only those proton pulses having an amplitude above the fast discriminator threshold were examined for coincidence with the γ-ray signal. The peaks labeled (O), (C), and (1) are, respectively, the oxygen elastic peak, the carbon elastic peak, and the first excited peak in ^{56}Fe at 0.847 MeV. (b) Spectrum of all rays in coincidence with the proton group leading to the first excited state in ^{56}Fe.

[10] W. H. Barkas and M. J. Berger, in *Studies in Penetration o Charged Particles in Matter* (Printing and Publishing Office, National Academy of Sciences–National Research Council, Washington, D.C. 20025, 1964), p. 103.

experimental stopping-power and range data in terms of Z and mean atomic excitation energy I. Uncertainty in the measured energy loss was combined with the standard error of the fit and uncertainty in I to give 3.4% standard error for the value of nuclei/cm^2, assuming the target was uniform over the beam-spot size. However, target nonuniformity could give rise to additional uncertainty. Proton energy losses at other bombarding energies were derived from the same range-energy relation; for excitation functions a simpler stopping-power formula was used.[11] Several target geometries were used. For the higher-resolution excitation functions, the thin foil was oriented with the angle between the beam and the target normal $\theta_t=0°$, giving a proton energy spread at 5 MeV of $\Delta E_p=$ 42 keV; for correlation measurements the heavier foil was used with $\theta_t=55°$, giving $\Delta E_p=193$ keV; for angular distribution the heavier foil was oriented at $\theta_t=0°$ and $\theta_t=45°$.

Antipileup circuit. Particle-detector current pulses were fed through a time pickoff unit to a charge-sensitive preamplifier. Fast γ-ray signals were obtained by clipping the amplified RCA 8054 anode pulses; a linear signal was taken from the ninth dynode. These four pulses were used in fast-slow coincidence, as shown schematically in Fig. 1. The arrangement is conventional, except that antipileup techniques described by Blatt *et al.*[12] were incorporated in the γ-ray channel, where rates exceeded 10^4 counts/sec. At this rate about 4% of the double-delay–line-shaped linear pulses were pileup-distorted. For this reason crossover timing was not used.[13] The ratio of true to accidental coincidence counts was $\sim$5:1, with a resolving time of 55 nsec.

The antipileup method is briefly described here to outline its application to correlation measurements; a more general discussion is given in Ref. 4. Two fast integral discriminators in Fig. 1 are labeled HI and LO. Only linear signals whose corresponding fast pulses passed HI were considered for analysis; pulses passing LO were those whose linear signals were large enough to cause pileup. Also shown is a gate-and-delay generator (GDG), which produced an output pulse 4 μsec after a start pulse, provided no stop pulse arrived during that time. This output pulse signified that the corresponding linear signal was not piled up. During the conditional 4 μsec the fast channel was inspected, by means of the LO discriminator, for other pulses which might have occurred near the pulse of interest. The 3-μsec delay in the stop channel permitted inspection from 3 μsec before to 1 μsec after the pulse of interest; only a pulse in this period would distort the double-delay–line-shaped linear signal of interest. Pulses passing HI also passed LO; the gate after LO simply prevented the self-stopping of each HI. The 4-μsec dead time in the start channel provided for pileup rejection of the third pulse in the following set of three consecutive start pulses, with times in μsec: $t_1=0$, $1<t_2<3$, and $4<t_3<7$.

Data reduction. Figure 2(a) is a particle spectrum representative of the angular distribution data. The mean bombarding energy was 5.00 MeV, the detector was at 90°, and the target-foil orientation was 45° with respect to the beam. The particle groups are identified. The counting rate was reduced by the use of an upper-level discriminator which removed all of the ^{56}Fe elastic peak. For (triple) correlation measurements, a single-channel analyzer was set around the ^{56}Fe inelastic peak; the resulting gated NaI(Tl) spectrum is shown in Fig. 2(b). The separately routed accidentals (6% in this case) were subtracted.

Photopeak area extraction was straightforward for the single-line NaI spectra. The particle spectra, however, required careful corrections for elastic contaminants at several angles greater than 100°. These corrections were based on published[14] relative angular distributions for elastic scattering and were less than 15% except for the highest bombarding energy, where back-angle corrections were near 30%. These corrections are reflected in the larger uncertainties associated with angular distribution cross sections near 150°.

All data were corrected for the calculated Rutherford scattering loss of collected beam due to the finite acceptance angle of the Faraday cup; this correction was near 2% for angular distributions and correlations, reaching 5% only for the thick-target excitation function. All results have been converted to center-of-mass cross sections and detection angles, while the bombarding energies quoted are average laboratory energies, denoting the proton energy at the center of the target foil.

Uncertainties. Total fractional uncertainties are shown in Figs. 4–6 as error bars. These are relative standard errors which are the result of combining uncertanties due to the following: (1) statistical errors, (2) peak area extraction methods, and (3) normalization required by the different target-foil orientations for some particle detection angles. In addition to these are the following known significant systematic uncertainties: for the angular distributions, 4%, due to uncertainties in nuclei/cm^2 and particle-detector solid angle; for triple correlations, 4%, due to uncertainties in nuclei/cm^2 and the NaI detector efficiency. The estimated standard error for excitation function normalization is about 8%.

[11] W. Whaling, in *Handbuch der Physik*, edited by S. Flügge (Springer-Verlag, Berlin, 1958), Vol. 34, p. 13.
[12] S. L. Blatt, J. Mahieux, and D. Kohler, Nucl. Instr. Methods **60**, 221 (1968).
[13] S. L. Blatt, Nucl. Instr. Methods **49**, 235 (1967).
[14] G. G. Shute, D. Robson, V. R. McKenna, and A. T. Berztiss, Nucl. Phys. **37**, 535 (1962); G. Hardie, R. L. Dangle, and L. D. Oppliger, Phys. Rev. **129**, 353 (1963).

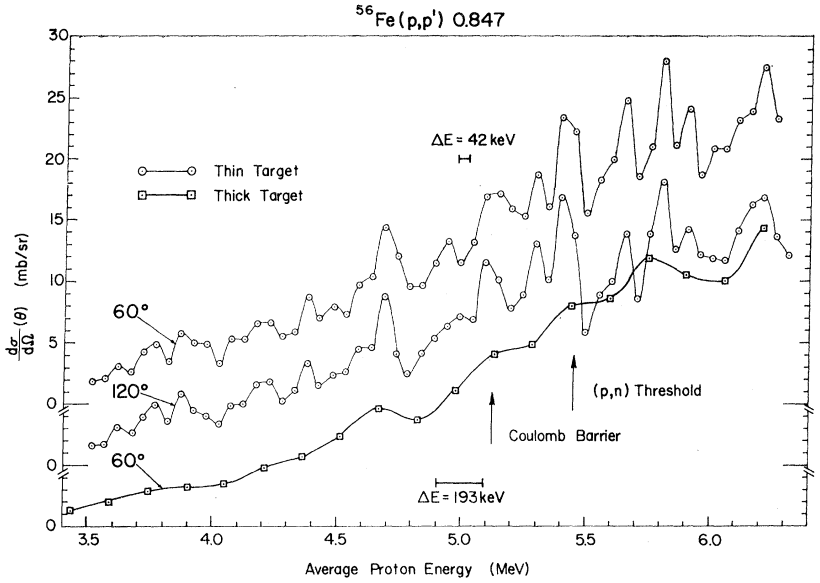

FIG. 3. Excitation function from 3.5 to 6.2 MeV for protons inelastically scattered from ^{56}Fe. The upper two curves follow data taken with an isotopically enriched target which was 42 keV thick at 5 MeV. Open squares denote data taken with an isotopically enriched target of 193-keV thickness at 5 MeV. Thin-target data are shown for scattered proton angles of 60° and 120°; thick-target data are shown for 60°. The scales of the curves have three separate zeros which are displaced by 5 mb/sr. The solid lines through the experimental points serve only to guide the eye and are not calculated fits to the curves.

III. RESULTS

A. Yield Curves

Elastic and inelastic yield curves for protons on ^{56}Fe were measured over the bombarding energy range of interest at two supplementary (c.m.) angles, 60° and 120°, and for two target thicknesses. The inelastic results are shown in Fig. 3.

If the statistical assumptions were met for this reaction, then one would have expected that the yield curve (both elastic and inelastic) would have a rather smooth energy dependence. Any "bumps" in the yield curve could possibly be associated with level-density fluctuations of the Erickson[15] type. An examination of Fig. 3 reveals that there are many resonantlike bumps in the yield curve that persist at both angles. The widths of these bumps are typically on the order of the target energy spread. The resonancelike structure in the yield curves was averaged out experimentally by increasing the target thickness to 193 keV for 5.0-MeV protons, as shown in Fig. 3. There is little likelihood that this type of energy averaging satisfies the statistical CN type of zero average value for interferences between these gross states. However, there was no hope whatsoever of having the statistical CN theory predict such rapid fluctuations as were measured in the yield curve. The problems associated with the resonances in the yield curve will be treated further in Sec. V.

The yield curves were measured at two supple-

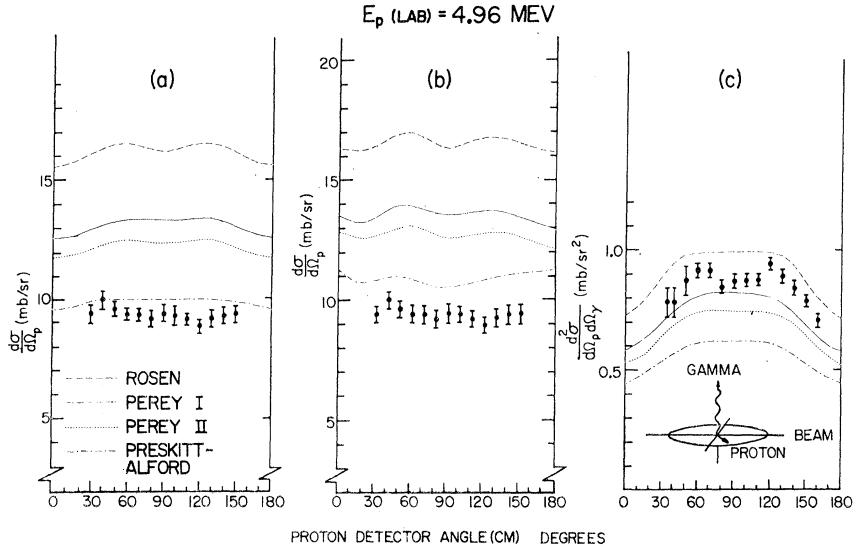

FIG. 4. Experimental points in (a) and (b) are the results of the angular distributions of protons leaving the residual ^{56}Fe nucleus in its first excited state at 0.847 MeV. The bombarding energy is 4.96 MeV. Experimental points in (c) are the particle–γ-ray angular correlations measured in the spin-flip geometry. The various curves on the figures are cross sections calculated using different sets of optical-model parameters as described in the text. The calculated curves in (a) are CN calculations alone, the curves in (b) are the incoherent sum of CN and DI calculations, and the curves in (c) are CN calculations.

[15] T. Erickson, Ann. Phys. (N.Y.) **23**, 390 (1963).

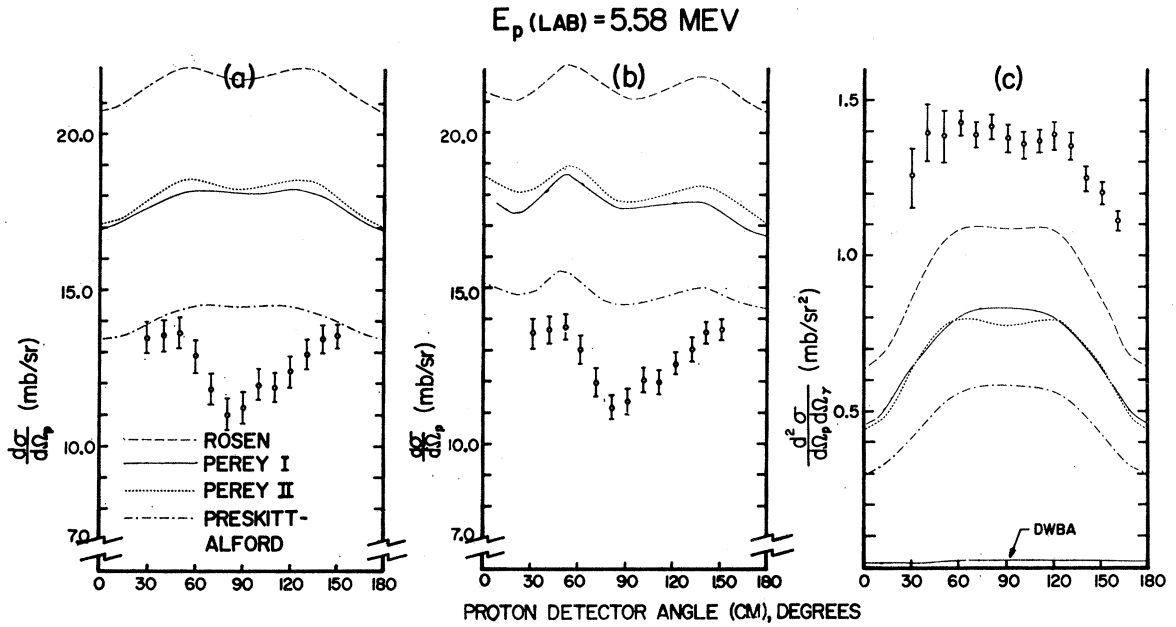

FIG. 5. Same as Fig. 4, except that E_p(lab) = 5.58 MeV. The DI calculation of the spin-flip cross section is shown in (c) and marked DWBA.

mentary (c.m.) angles in order to check the validity of the statistical CN prediction that

$$\frac{d\sigma}{d\Omega_p}(\theta_p, \phi_p) = \frac{d\sigma}{d\Omega}(\pi - \theta_p, \phi_p).$$

This prediction appears to be valid up to a bombarding energy of 5.0 MeV. Above this bombarding energy, the cross section for the forward-scattering angle becomes larger than for the backward-scattering angle. These results are consistent with the data of Ref. 1 for inelastic scattering of protons from ^{48}Ti and are interpreted as being evidence for the onset of a DI component to the reaction.

B. Angular Distributions and Angular Correlations

The results of the angular distributions of protons scattered inelastically from ^{56}Fe, leaving the residual nucleus in its first 2^+ excited state at 0.847 MeV, are

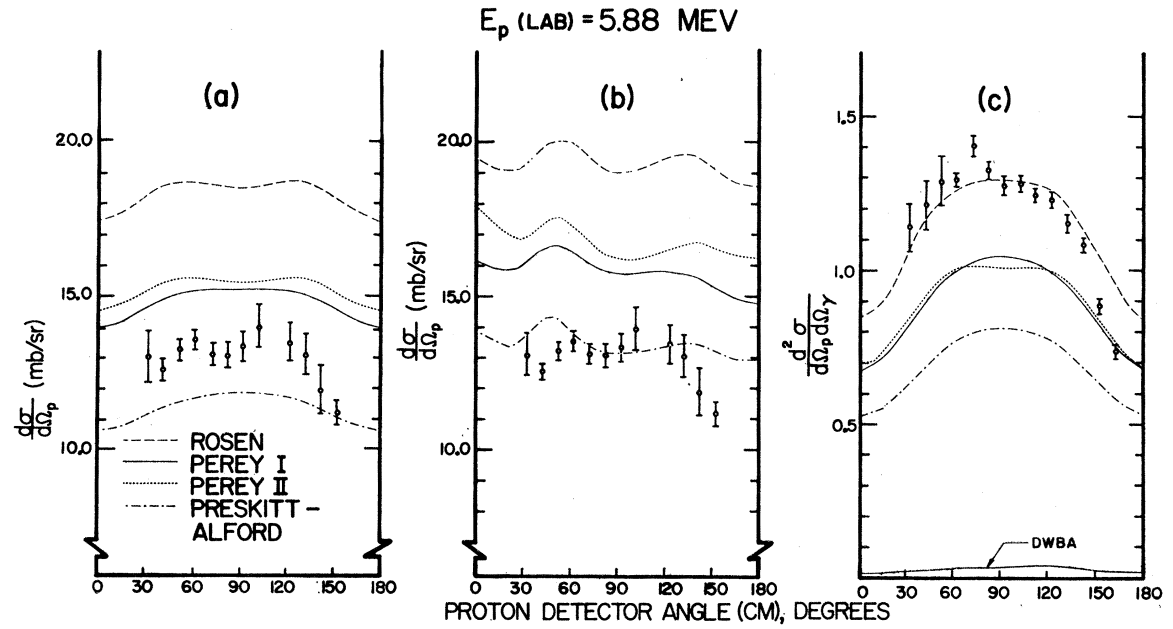

FIG. 6. Same as Fig. 5, except that E_p(lab) = 5.88 MeV.

shown in Figs. 4–6. Measurements of the angular distributions were made at three bombarding energies. The same experimental points are plotted twice in each figure to facilitate comparisons with the theoretical calculations. The angular distributions were measured as absolute cross sections. The proton energy values on the figures are the values for the angular correlation experiments. For angular distributions, the proton bombarding energies, corrected to the value at half-target thickness, are approximately 40 keV larger than the half-target values used in the angular correlations.

Angular correlations between the inelastically scattered protons and the 0.847-MeV γ rays from the decay of the first excited 2^+ state in ^{56}Fe were measured with the γ-ray detector fixed along a direction perpendicular to the reaction plane (the "spin-flip" geometry). The results of the angular correlations, measured as absolute double-differential cross sections, are shown in Figs. 4–6. The angular correlations were measured at approximately the same proton bombarding energies as those used to measure the proton differential cross sections. Determination of the experimental uncertainties associated with the measured distributions and correlations is described in Sec. III.

The results of the measured spin-flip probabilities are shown in Fig. 7. For these data we have corrected for the small (but finite) contribution of the radiations from the $m=\pm 2$ and $m=0$ substates, which contribute radiation due to the finite size of the γ-ray detector, according to the prescription developed by Schmidt *et al.*[9]

IV. CALCULATIONS

A. Statistical CN Analysis

The directional correlation function for inelastic nucleon scattering by means of the statistical CN reaction mechanism has been developed by Satchler[16] and generalized to include a spin-orbit interaction by Sheldon.[17] Using the ALGOL language, Sheldon and Gantenbein[18] have written a computer program entitled BARBARA, which computes this function, describing the directional correlation between the inelastically scattered nucleon and the deexcitation γ ray emitted by the residual nucleus. This code has been slightly amended to incorporate the calculation of the proton angular distribution and spin-flip probability. The results of calculations of proton angular distributions and angular correlations, using four different sets of optical-model parameters, are shown in Figs. 4–6.

As part of the input for the code BARBARA, one must supply the penetrabilities or transmission coefficients of the various partial waves. These energy-dependent transmission coefficients may be obtained with the aid of the optical model. We used the optical-model program of Auerbach called ABACUS-II.[19] For the real nonspin-dependent part of the nuclear potential, we employed the usual Woods-Saxon form factor, for the imaginary part the derivative of a Woods-Saxon form, and for the spin-orbit part the familiar Thomas form.

Since some of the incident proton energies were above the (p, n) threshold, it was necessary to obtain neutron as well as proton transmission coefficients. For the neutron penetrabilities, we used at each energy the local potential equivalent to the nonlocal-neutron optical model of Perey and Buck.[20] We used the local potential only because the code ABACUS-II has no provision for use of a nonlocal potential. The neutron (local) optical-model parameters used were $V=48-0.29E$, $W=10$, $r_0=r_0'=1.25$, $a=0.65$, and $a'=0.47$, in the notation of Ref. 24, where the energies are in MeV and the lengths in F. The depth of the (real) spin-orbit potential was taken as 7.5 MeV, which is close to the value used by Perey and Buck in their nonlocal neutron potential.

The proton penetrabilities were calculated using four different sets of optical-model parameters. One set, called Perey I, was obtained by extrapolating the proton (local) optical-model parameters of Perey,[21] which he obtained by fitting proton elastic scattering data in the 9–12-MeV energy range. A second set of parameters, called Perey II, was obtained from the same original data in the 9–12-MeV energy range. However, for this second set, a better fit was ob-

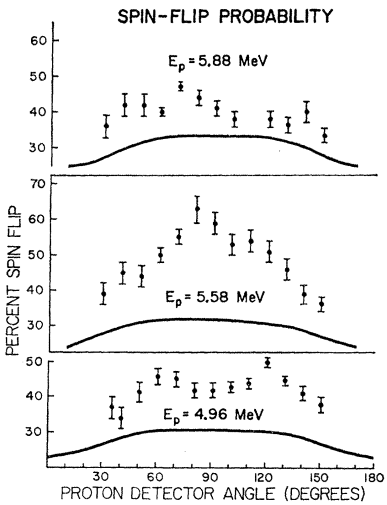

FIG. 7. Spin-flip probability, as described in the text, plotted at three bombarding energies. The solid curves are the spin-flip probabilities calculated using only the CN contribution.

[16] G. R. Satchler, Phys. Rev. **94**, 1304 (1954); **104**, 1198 (1956).
[17] E. Sheldon, Rev. Mod. Phys. **35**, 795 (1963).
[18] E. Sheldon and P. Gantenbein, Z. Angew. Math. Phys. **18**, 397 (1967).
[19] Written by E. Auerbach (obtained from Brookhaven National Laboratory, Upton, N.Y.).
[20] F. Perey and B. Buck, Nucl. Phys. **32**, 353 (1962).
[21] F. Perey, *Direct Interactions and Nuclear Reaction Mechanisms* (Gordon and Breach, Science Publishers, Inc., New York, 1963).

TABLE I. Summary of optical-model parameters used for determination of proton penetrabilities for the statistical CN calculations.

Source	V (MeV)	W (MeV)	r_0 (F)	a (F)	a' (F)	V_s (MeV)
Perey I[a]	$53.3-0.55E+0.4ZA^{-1/3}+27(N-Z)/A$	11	1.25	0.65	0.47	7.5
Perey II[a]	$46.7-0.32E+ZA^{-1/3}$	11	1.25	0.65	0.47	7.5
Rosen[b]	$53.8-0.33E$	7.5	1.25	0.64	0.70	5.5
Preskitt-Alford[c]	55.0	5.0 (volume)	1.37	0.4	0.4	5.0

[a] Reference 21.
[b] Reference 22.
[c] Reference 23.

tained to the first minimum of the angular distributions by disregarding the back-angle data. It was assumed that the explicit energy dependence would permit the use of these parameters at even lower energies.

A third set of optical-model parameters used was obtained by extrapolating the published parameters of Rosen[22] from his analysis of the polarization data at an energy of 7 MeV. The fourth set of optical-model parameters used was obtained from the work of Preskitt and Alford,[23] who obtained their parameters by fitting the elastic scattering of protons on Fe for energies between 3.5 and 6.5 MeV, which includes the energy range studied in the present work. The Preskitt-Alford parameters were changed slightly to include a spin-orbit potential. A listing of the various optical-model parameters used is included in Table I.

B. Direct-Reaction Contributions

The direct-reaction contribution was calculated in the distorted-wave Born approximation (DWBA) utilizing the collective-model extension of the optical model to include nonspherical potentials.[24,25] Inelastic scattering to collective vibrational or rotational states is then induced by the nonspherical parts of the potentials. These were included in the present work only to first order in the multipole deformation parameter β_l. An especially attractive feature of this interaction is the fact that the parameters, except for the deformation β_l, may, at least in principle, be determined from the elastic scattering (spherical optical model).

This model has recently been employed by Fricke, Gross, and Zucker[26] for the analysis of their 40-MeV polarized proton inelastic scattering data. These Oak Ridge calculations included four contributions to the form factor representing the inelastic interaction. These contributions are first-order terms in β due to four nonspherical potentials: the real central nuclear potential, the Coulomb potential, the imaginary central nuclear potential, and the spin-orbit potential. The deformed spin-orbit potential is comparatively complicated; accordingly, the Oak Ridge group treated it in the approximation that only the radial derivative part of the gradient operator is important. After they had made this simplification, it seemed only reasonable to permit β^{so}, the deformation associated with the spin-orbit potential, to differ from the deformation β associated with the other parts of the optical potential. Indeed, they found a consistent preference for the ratio β^{so}/β to be between 1 and 2.

Sherif and Blair[27] have extended the treatment of the deformation of the spin-orbit potential by including the angular derivatives, thereby fully treating the Thomas term. For proton energies above 29 MeV and for scattering angles less than 60°, they find substantial improvement in asymmetries when employing the full Thomas term. Curiously, even with full treatment, the tendency of the ratio β^{so}/β to exceed 1 persists. At 18.6 MeV, the situation is less clear, in that they find that the use of the full Thomas term does not necessarily improve the fit to the asymmetry data. The latter conclusion appears to hold at even lower energy, viz., between 10 and 15 MeV, where the proton spin-flip probability measurements of Kolasinski[28] were compared with preliminary calculations of Blair and Sherif (see, e.g., Fig. 31 of Ref. 28).

For the present work, the DWBA calculations were performed using the code JULIE.[25] The spin-orbit deformation was treated in the same approximation as in the Oak Ridge calculations described above. More specifically, the detailed form of the inelastic interaction was taken to be that of Eq. (12) in Ref. 26.

[22] L. Rosen, J. G. Beery, A. S. Goldhaber, and E. H. Auerbach, Ann. Phys. (N.Y.) **34**, 96 (1965).
[23] C. A. Preskitt and W. P. Alford, Phys. Rev. **115**, 389 (1959).
[24] R. H. Bassel, G. R. Satchler, R. M. Drisko, and E. Rost, Phys. Rev. **128**, 2693 (1962).
[25] G. R. Satchler, Nucl. Phys. **55**, 1 (1964).
[26] M. P. Fricke, E. E. Gross, and A. Zucker, Phys. Rev. **163**, 1153 (1967).
[27] H. Sherif and J. S. Blair, Phys. Letters **26B**, 489 (1968).
[28] W. A. Kolasinski, Ph.D. thesis, University of Washington, 1967 (unpublished).

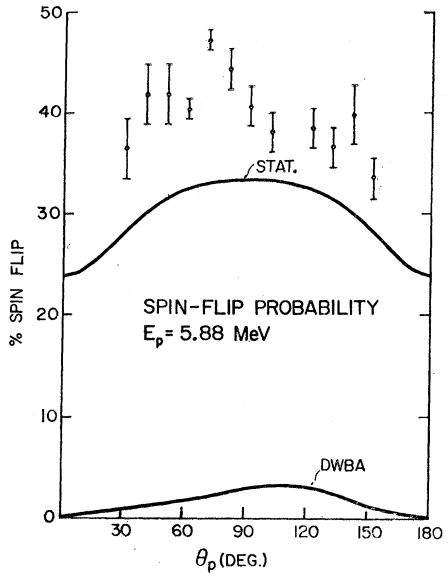

FIG. 8. Experimental values of spin-flip probability, as measured at E_p(lab) = 5.88 MeV, shown in order to compare with the predictions of the CN and DI model calculations.

Thus, the Coulomb excitation process was included in the present analysis. This excitation process was neglected in the Sherif-Blair calculations. Their comparison with the Oak Ridge calculations indicated that the inclusion of Coulomb excitation is important for the magnitude of cross sections but not for computing asymmetries.

Values of the deformation parameter β_2 for the 0.847-MeV (2^+) state of ^{56}Fe have been obtained from a variety of experimental studies, such as the inelastic scattering of ^{3}He particles[29] and protons,[30] as well as Coulomb excitation using α particles[31] and heavy ions.[32] The β_2 values obtained in these studies range from 0.19 to 0.24, typically with 10% error estimates. We have treated β_2 as known and have fixed its value at 0.24. The only remaining input parameters were the usual optical-model constants and the ratio β_2^{so}/β_2. On the basis of the higher-energy calculations already mentioned, this ratio might be expected to lie between 1 and 2. However, lacking knowledge as to the energy variation of the ratio, we have arbitrarily set the ratio equal to 1 for our calculations. The DWBA contributions were calculated at the three bombarding energies for each of the optical-model parameter sets which were used in the statistical-model calculations.

[29] E. R. Flynn and L. Rosen, Phys. Rev. **153**, 1228 (1967).
[30] J. Benveniste, A. C. Mitchell, B. Buck, and C. B. Fulmer, Phys. Rev. **133**, B323 (1964).
[31] G. M. Temmer and N. P. Heydenburg, Phys. Rev. **104**, 967 (1956).
[32] H. E. Gove and C. Broude, in *Reactions between Complex Nuclei*, edited by A. Zucker, F. T. Howard, and E. C. Holbert (John Wiley & Sons, Inc., New York, 1960), p. 57; B. M. Adams, D. Eccleshall, and M. J. L. Yates, *ibid.*, p. 95; D. Beder, Can. J. Phys. **41**, 547 (1963); D. G. Alkhazov, A. P. Grinberg, K. I. Erokhina, I. K. H. Lemberg, Izv. Akad. Nauk SSSR Ser. Fiz. **23**, 223 (1959).

V. DISCUSSION

In performing this experiment, our intent was to conduct measurements on a nuclear species for which, at moderate bombarding energies, the predicted level densities would be sufficiently large to make the statistical CN description a reasonable first approximation. It was recognized that direct-interaction processes could also be present. The goal was then to compare the experimental cross sections and angular correlations with values calculated using an incoherent superposition of CN and DI processes:

$$\frac{d\sigma}{d\Omega}(\theta_p) = \frac{d\sigma}{d\Omega_{\mathrm{CN}}} + \frac{d\sigma}{d\Omega_{\mathrm{DI}}}.$$

Incoherence between the CN and DI processes was a necessary assumption in order to remain within the spirit of the statistical model. The various optical-model parameters used for both the CN and DI calculations were obtained from the literature as described in Sec. IV.

Comparing the measured particle angular distribution and angular correlations with the calculated values using only the CN contributions, one observes that none of the various sets of optical-model parameters gives rise to a fit to both the angular distributions and the angular correlations. This can be seen in parts (a) and (c) of Figs. 4–6. The CN calculations using the Preskitt-Alford optical-model parameters come closest among all the parameter sets to the measured particle angular distributions. However, the CN-calculated spin-flip correlations using these same parameters underestimate the measured correlation by a factor of 2 at the higher bombarding

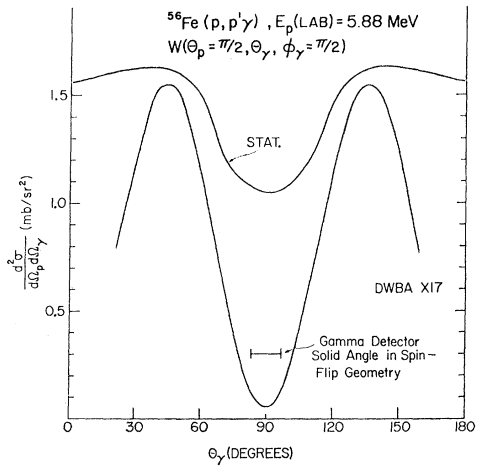

FIG. 9. Calculated values of the particle–γ-ray angular correlations in the geometry in which the γ-ray detector moves in a plane perpendicular to the reaction plane and contains the beam direction. In a coordinate system where the z axis is along the incident beam direction and the x axis is in the reaction plane, the spin-flip geometry is the one wherein $\phi_\gamma = \theta_\gamma = \frac{1}{2}\pi$. The plotted curves are the predicted angular distributions of the particle–γ-ray correlations calculated from the CN and DI models.

energies. Conversely, the Rosen optical-model parameters appear to give the best fit among all the parameter sets to the observed correlations, but overestimate the particle angular distributions by a factor of about 2. It should be emphasized that, in each case, the optical-model parameters have been extrapolated from data fitted at somewhat higher energies. Still, one would have hoped to find consistency between the calculations based upon the various extrapolated parameters and better agreement between the calculated values and the present experimental data.

As described in Sec. IV, angular distributions and spin-flip angular correlations were also calculated in the DI formalism using the same four sets of optical-model parameters as those used for the CN calculations. The results of the calculated DI angular distributions were added incoherently to the CN-calculated angular distributions, and the results are displayed in Figs. 4(b), 5(b), and 6(b). The magnitude of the calculated DI angular distributions is approximately 15% of the magnitude of the calculated CN angular distributions at the highest energy of $E_p=5.88$ MeV. Moreover, the calculated DI spin-flip correlation contributions were, at the most, 4% of the calculated CN spin-flip correlations. The calculated CN and direct spin-flip probabilities are compared with the measured values in Fig. 8.

In order to investigate the reason for the small DI spin-flip correlation prediction, we computed the directional correlation function for a geometry in which the γ-ray detector moves in a plane perpendicular to the reaction plane (hereafter referred to as a perpendicular correlation). The results of this calculation are shown in Fig. 9, along with the corresponding CN calculation using the same set of optical-model parameters. The DI perpendicular correlation shows a very strong angular dependence. The cross section in the spin-flip geometry is found to be more than an order of magnitude smaller than the peak value of the cross section (at about $\theta_\gamma=40°$). In contrast, the CN perpendicular correlation shows approximately a 3:2 ratio from peak to valley. Because of the strong angular dependence of the perpendicular correlations, the finite size of the γ-ray detector may introduce large corrections in reactions dominated by the DI mechanism. The finite size of the γ-ray detector was included in the calculated DI spin-flip correlations shown in Figs. 5(c) and 6(c).

The calculated CN spin-flip probabilities are shown in Fig. 7, along with the measured spin-flip probabilities. The calculated CN spin-flip probabilities are nearly the same for all four optical-model parameter sets and predict a maximum spin-flip probability of approximately 33%. Calculated DI spin-flip probabilities over the same energy range show a maximum contribution of about 4%. Whereas the CN spin-flip probabilities show symmetry about $\theta_p=\frac{1}{2}\pi$, the DI contributions exhibit a slightly backward peaking. At proton bombarding energies of 15 to 20 MeV, Schmidt *et al.*[33] have reported spin-flip probabilities on the order of 30%, but strongly backward-peaked. Their data on C^{12} and ^{58}Ni are compared with a DWBA calculation, and reasonable fits are obtained. However, calculations by Richter and Parish[34] on CN effects in (p, n) charge-exchange reactions on light nuclei show evidence of CN contributions to inelastic proton scattering of as large as 40% at bombarding energies of 12 MeV. The magnitude and symmetry of the measured spin-flip correlations over the energy range of our investigations indicate a dominant CN contribution.

A possible explanation for the limited agreement between the measured and calculated cross sections and correlations may reside in the resonancelike structure observed in the yield curve. There is no mechanism in the statistical CN model to account for this structure. Hence, the observed differences between calculations and measurements may be related to the existence of such a structure. On the other hand, it is difficult to understand why effects of this type would influence the behavior in the same way at each of the three energies of this experiment.

We have measured the elastic and inelastic yields for the ^{56}Fe plus proton reaction at a number of proton detector angles and over the energy range of this experiment. For the inelastic channel, leaving the residual nucleus in its first excited state of 0.847 MeV, the resonances observed in Fig. 3 persist over all proton detector angles and indicate that these are not statistical fluctuations. Currently, we are investigating this resonancelike behavior using a 5-keV-thick target in order to observe the existence of fine structure.

There is certainly a possibility that the observed resonances in the yield curve represent isobaric analog states of the nucleus ^{57}Fe. Should this be true, our assumption of incoherence in the reaction mechanisms would need modification. Analog resonance states of definite spin and parity could coherently interfere both with the nonresonant background and with direct-reaction processes. Interference of this nature may explain the differences between our measured and calculated cross sections.

Although there are significant differences between the observed angular distributions and spin-flip correlations and the values computed using the CN statistical formalism, the CN calculations do give the correct order of magnitude. The calculated DI contributions, on the other hand, are quite small over this energy range. Because of the lack of good agreement between the measured cross sections and the CN-calculated cross sections, we were unable to extract quantitatively the DI contribution to the reaction using the assumptions of incoherence between reaction mechanisms.

---

[33] F. H. Schmidt *et al.*, University of Washington Nuclear Physics Laboratory Annual Report, 1968, p. 82 (unpublished).

[34] A. Richter and L. J. Parish, Phys. Rev. Letters **21**, 1824 (1968).